

Volodymyr Baran and Thomas F. Fässler*

Li vs. Zn substitution in $\text{Li}_{17}\text{Si}_4$ – $\text{Li}_{17-\varepsilon-\delta}\text{Zn}_\varepsilon\text{Si}_4$ connecting the structures of $\text{Li}_{21}\text{Si}_5$ and $\text{Li}_{17}\text{Si}_4$

<https://doi.org/10.1515/znb-2019-0157>

Received October 3, 2019; accepted October 23, 2019

Abstract: Binary lithium silicides play a crucial role in high energy density anode materials for rechargeable batteries. During charging processes of Si anodes $\text{Li}_{15}\text{Si}_4$ is formed as a metastable phase which has been stabilized through Li by Mg, Zn and Al substitution. Here we investigate Li by Zn substitution in the lithium-richest phase $\text{Li}_{17}\text{Si}_4$ and report on the particular site preference of Zn atoms since Zn is substituting Li atoms only on one out of 13 possible lithium sites. This site preference shows an interesting relation to the closely related phase $\text{Li}_{21}\text{Si}_5$ and thus $\text{Li}_{17-\varepsilon-\delta}\text{Zn}_\varepsilon\text{Si}_4$ with $\varepsilon = 0.025(1)$ and $\delta = 0.033(1)$ can be considered as the missing link between the structures of $\text{Li}_{21}\text{Si}_5$ ($= \text{Li}_{4.20}\text{Si}$) and $\text{Li}_{17}\text{Si}_4$ ($= \text{Li}_{4.25}\text{Si}$).

Keywords: crystal structure; lithium; silicon; synthesis.

Dedicated to: Professor Arndt Simon on the occasion of his 80th birthday.

1 Introduction

Nowadays lithium-ion batteries (LIBs) are widely used as rechargeable power cell for electronic devices. Lithium intercalation of the anode is one of the important processes in lithium ion batteries. Due to its rather high theoretical lithium capacity, silicon is one of the promising candidates for anode materials in LIBs. Silicon anodes exhibit a more than one order of magnitude larger capacity (4200 mA h g⁻¹ for $\text{Li}_{17}\text{Si}_4$) than currently used graphite anodes (372 mA h g⁻¹) [1, 2].

Several phases are observed at the lithium-rich side of the binary phase diagram. These are $\text{Li}_{17}\text{Si}_4$, $\text{Li}_{21}\text{Si}_5$, the

high-temperature phase $\text{Li}_{16.44}\text{Si}_4$ and meta-stable $\text{Li}_{15}\text{Si}_4$. None adapts to a composition appropriate for an electron-precise Zintl phase. For a valence-precise compound with isolated Si atoms a ratio of Li to Si of 4:1 is expected according to the formal charge transfer $(\text{Li}^+)_4(\text{Si}^{4-})$ or $\text{Li}_{16}\text{Si}_4$. Most intriguing is meta-stable $\text{Li}_{15}\text{Si}_4$ which is, according to the Zintl formalism, short by one cation to charge balance 16 negative charges of four Si^{4-} . However, meta-stable $\text{Li}_{15}\text{Si}_4$ transforms to thermodynamically stable phases by substituting Li by more electron rich electropositive elements. For $\text{Li}_{15}\text{Si}_4$ we found a stabilization through Li by Mg, Zn, and Al substitution and formation of $\text{Li}_{14}\text{MgSi}_4$, $\text{Li}_{14.05}\text{Zn}_{0.95}\text{Si}_4$ and $\text{Li}_{14.25}\text{Al}_{0.75}\text{Si}_4$, respectively [3, 4].

Recently $\text{Li}_{17}\text{Si}_4$ has been established as the lithium-richest phase in course of a detailed investigation of the Li-rich side of the binary phase diagram and allowed for a very accurate structure determination [5]. This revealed significant differences to previously reported $\text{Li}_{21}\text{Si}_5$ [6] to which it is very close in composition ($\text{Li}_{17}\text{Si}_4 = \text{Li}_{4.25}\text{Si}$, $\text{Li}_{21}\text{Si}_5 = \text{Li}_{4.20}\text{Si}$). Interestingly, no substantial phase width is reported for any of these phases.

In this context we also investigated the partial substitution of Li by Zn in $\text{Li}_{17}\text{Si}_4$ and report here on the particular site preference of the Zn atoms.

2 Experimental section

2.1 Synthesis

Li flux syntheses were performed as described in the literature [3, 5]. Stainless-steel ampoules with a filter placed inside were also adapted from the literature [7]. A total mass batch of 0.5 g contained the molar ratios of the elements Li:Zn:Si = 17:1:3. Si and Zn powder were pressed into a pellet, which was loaded into the ampoule between Li pieces. The ampoules were sealed by arc welding and placed in a steel cylinder with silica wool inside. The cylinder was located in a muffle furnace (Nabertherm, Controller P330/B180), heated to $T = 750^\circ\text{C}$ with a rate of 3 K min⁻¹ and held at this temperature for 1 h. Afterwards the sample was cooled to 450°C at a rate of 5 K h⁻¹ and kept at this temperature for 4 days. Excess Li was removed at this temperature by isothermal centrifugation. After

*Corresponding author: Thomas F. Fässler, Department Chemie, Technische Universität München, Lichtenbergstraße 4, D-85747 Garching, Germany, Fax: (+49) 89-289-13186, E-mail: thomas.faessler@lrz.tum.de.

homepage: <https://www.department.ch.tum.de/acnm/>

Volodymyr Baran: Heinz Maier-Leibnitz Zentrum (MLZ), ZWE FRM II, Technische Universität München, Lichtenbergstraße 1, D-85748 Garching, Germany

cooling to room temperature, the ampoule was opened inside a glove box and the product was recovered as shiny crystals reaching a few millimeters in size. Most of the crystals were located on the top of the filter and some stacked to the wall at the bottom of the ampoule.

2.2 Energy-dispersive X-Ray spectroscopy (EDX)

To confirm the composition of $\text{Li}_{17-\epsilon-\delta}\text{Zn}_\epsilon\text{Si}_4$ a JEOL-JSM 7500F scanning electron microscope equipped with an Oxford X-Max EDX analyzer was used with Mn as internal standard. Si was detected as the main element. The Zn signals were clearly observed, and the content was below 1 at.% (see Figure S2, Supporting Information available online).

2.3 X-ray crystallography

The PXRD pattern of $\text{Li}_{17-\epsilon-\delta}\text{Zn}_\epsilon\text{Si}_4$ obtained from grinded single crystals was indexed with an *F*-centered cubic cell and perfectly matches with the recently discovered $\text{Li}_{17}\text{Si}_4$ structure model [5] (see Figure S1, Supporting Information available online). The slightly but significantly enlarged unit cell parameter $a=18.7441(3)$ Å indicates the partial substitution of Li by Zn, if compared to the binary system $\text{Li}_{17}\text{Si}_4$ (18.7259(2) Å, $\text{Li}_{17}\text{Sn}_4$ structure type) [8]. Single crystals were selected and cut in an Ar-filled glove box and placed inside a glass capillary which was subsequently sealed. Intensity data was collected at $T=123$ K and at room temperature. Low-temperature measurements were performed on a Bruker APEX II X-ray diffractometer equipped with a CCD detector, a fine focused sealed tube with $\text{MoK}\alpha$ radiation ($\lambda=0.71073$ Å) and a graphite monochromator. The data collection process was controlled with the Bruker APEX Software suite [9]. Integration, data reduction, and absorption correction were performed with the programs SAINT and SADABS [10, 11].

The crystal structure was solved by Direct Methods (SHELXS-97) [12] and refined with full-matrix least-squares calculations on F^2 (SHELXL-2014/7) [13]. Fractional atomic coordinates and atomic displacement parameters for mixed Li/Zn sites were set equal. Details of the single-crystal structure investigation are given in Tables 1–3.

Further details of the crystal structure investigation may be obtained from Fachinformationszentrum Karlsruhe, D-76344 Eggenstein-Leopoldshafen, Germany (fax: (+49) 7247-808-666; e-mail: crysdata@fiz-karlsruhe.de) on quoting the depository number CSD-1788919 ($\text{Li}_{16.942}\text{Zn}_{0.025}\text{Si}_4$).

Table 1: Crystallographic data and data collection and structure refinement parameters for $\text{Li}_{17-\epsilon-\delta}\text{Zn}_\epsilon\text{Si}_4$.

Empirical formula	$\text{Li}_{16.942(1)}\text{Zn}_{0.025(1)}\text{Si}_4$
Formula weight, g mol ⁻¹	231.54
<i>T</i> , K	123(2)
Diffractometer	APEX II
Radiation; wavelength, Å	$\text{MoK}\alpha$, 0.71073
Space group	$F\bar{4}3m$
<i>Z</i>	20
Unit cell dimension <i>a</i> , Å	18.637(2)
<i>V</i> , Å ³	6473.4(13)
$\rho_{\text{calcd.}}$, g cm ⁻³	1.19
Crystal size, mm ³	0.2 × 0.15 × 0.15
Absorption correction	Multi scan
μ , mm ⁻¹	0.4
<i>F</i> (000), <i>e</i>	2151
θ range, °	1.89–41.76
Reflections collected	40 780
Independent reflections	2214
$R_{\text{int}}/R_{\text{a}}$	0.0355/0.0158
Reflection with $I > 2\sigma(I)$	1985
Data/refined parameters	2214/70
Final indices R_1/wR_2 [$I > 2\sigma(I)$]	0.023/0.054
Indices R_1/wR_2 (all data)	0.030/0.057
Goodness-of-fit on F^2	1.083
Weight parameters <i>a/b</i> ^a	0.0238/3.6014
Flack parameter	0.56(7)
Largest diff. peak/hole, e Å ⁻³	0.89/–0.33

^a $W=[\sigma^2(F_o^2)+(aP)^2+bP]^{-1}$, where $P=[\text{Max}(F_o^2, 0)+2F_c^2]/3$.

3 Results and discussion

Single crystals of $\text{Li}_{17-\epsilon-\delta}\text{Zn}_\epsilon\text{Si}_4$ were obtained through Li flux syntheses by using the atomic ratio Zn:Si of 1:3 and Li removal at high temperature by isothermal centrifugation. Diffraction intensities were indexed in space group $F\bar{4}3m$ which is non-centrosymmetric, and therefore inversion twinning of two enantiomorphic species was considered for the structure refinement of a single crystal. All Li atoms could be refined with anisotropic displacement parameters. In the unit cell there are 80 silicon atoms located at 24*g*, 24*f* and two 16*e* sites, and 340 Li atoms located at 13 independent atomic sites (four 48*h*, 24*g*, 24*f*, six 16*e*, and 4*a*). Only the Li13 site (4*a*) shows a significant statistically mixed Li/Zn occupation (see Table 2). Careful inspection of the residual electron density revealed some density in the vicinity of Li7 (16*i*). Applying a split model for this position (Li7A and Li7B) led to unreasonably short Li7B–Li13 distances of 1.366(9) Å. Consequently the statistically mixed Li/Zn position which is not fully occupied remains empty in correlation with the occupation of Li7B (Fig. 1). The total s.o.f. for the Li13/Zn13 site was restricted to 0.832 (Table 2). The only short interatomic distance of 2.23(1) Å remains between two Li7B atoms

Table 2: Atomic coordinates and equivalent isotropic displacement parameters for $\text{Li}_{17-\delta}\text{Zn}_\delta\text{Si}_4$.

Atom	Wyckoff position	x/a	y/b	z/c	s.o.f.	$U_{\text{eq}} (\text{\AA}^2)$
Si1	24g	0.56986(2)	1/4	1/4	1	0.00695(8)
Si2	24f	0.32173(2)	0	0	1	0.00704(8)
Si3	16e	0.15998(1)	x	x	1	0.00590(8)
Si4	16e	0.91691(2)	x	x	1	0.00611(7)
Li1	48h	0.09057(9)	x	0.26272(11)	1	0.0154(5)
Li2	48h	0.09076(12)	x	0.76181(13)	1	0.0248(5)
Li3	48h	0.15515(8)	x	0.52068(12)	1	0.0179(4)
Li4	48h	0.16328(8)	x	0.00317(15)	1	0.0169(5)
Li5	24g	0.07547(17)	1/4	1/4	1	0.0143(6)
Li6	24f	0.16969(17)	0	0	1	0.0151(6)
Li7A	16e	0.07399(14)	x	x	0.832(7)	0.0087(6)
Li7B	16e	0.0423(5)	x	x	0.168(7)	0.0087(6)
Li8	16e	0.30266(10)	x	x	1	0.0140(5)
Li9	16e	0.41771(13)	x	x	1	0.0117(5)
Li10	16e	0.55766(10)	x	x	1	0.0122(5)
Li11	16e	0.68753(11)	x	x	1	0.0133(6)
Li12	16e	0.83197(13)	x	x	1	0.0186(8)
Li13/Zn13	4a	0	0	0	0.708/0.124(2) ^b	0.0063(5)

^a U_{eq} is defined as one third of the trace of the orthogonalized U_{ij} tensor. ^bSum of s.o.f. is restricted to 0.832.

Table 3: Anisotropic displacement parameters for $\text{Li}_{17-\delta}\text{Zn}_\delta\text{Si}_4$.

Atom	U_{11}	U_{22}	U_{33}	U_{12}	U_{13}	U_{23}
Si1	0.00727(15)	0.00679(10)	U_{22}	0	0	0.00015(12)
Si2	0.00623(14)	0.00745(10)	U_{22}	0	0	-0.00107(12)
Si3	0.00590(8)	U_{11}	U_{11}	0.00048(7)	U_{12}	U_{12}
Si4	0.00611(7)	U_{11}	U_{11}	0.00016(8)	U_{12}	U_{12}
Li1	0.0144(6)	U_{11}	0.0175(9)	-0.0027(7)	0.0047(5)	U_{13}
Li2	0.0261(8)	U_{11}	0.0221(11)	0.0004(10)	0.0036(6)	U_{13}
Li3	0.0193(6)	U_{11}	0.0152(8)	-0.0056(8)	-0.0013(5)	U_{13}
Li4	0.0168(6)	U_{11}	0.0169(9)	-0.0035(7)	0.0004(6)	U_{13}
Li5	0.0120(11)	0.0155(9)	U_{22}	0	0	-0.0103(11)
Li6	0.0158(12)	0.0148(8)	U_{22}	0	0	0.0038(12)
Li7A/Li7B	0.0087(6)	U_{11}	U_{11}	0.0032(7)	U_{12}	U_{12}
Li8	0.0140(5)	U_{11}	U_{11}	0.0003(6)	U_{12}	U_{12}
Li9	0.0117(5)	U_{11}	U_{11}	0.0012(6)	U_{12}	U_{12}
Li10	0.0122(5)	U_{11}	U_{11}	0.0014(6)	U_{12}	U_{12}
Li11	0.0133(6)	U_{11}	U_{11}	0.0035(6)	U_{12}	U_{12}
Li12	0.0186(8)	U_{11}	U_{11}	-0.0002(7)	U_{12}	U_{12}
Li13/Zn13	0.0063(5)	U_{11}	U_{11}	0	0	0

(Fig. 1e). The Li7A tetrahedron is occupied by a statistical Li/Zn mixture. The distances between the atoms Li13/Zn13 and Li7A are 2.388(3) Å (Fig. 1d) and thus slightly shorter than those reported for $\text{Li}_{17}\text{Si}_4$ (2.395(2) Å) [5]. This small difference can be explained by the fact that Zn has a smaller metallic radius than Li (1.57 Å for Li and 1.37 Å for Zn) [14]. The distances between the Li7A atoms are similar to those observed in $\text{Li}_{17}\text{Si}_4$ (3.900(4) Å comparing to 3.9101(16) Å). One could speculate that the 4a site is

occupied only by Zn atoms, but this would lead to an even bigger vacancy at 4a and does not correlate with the split of the Li7A-Li7B atoms.

The crystallographically determined composition is $\text{Li}_{16.942(1)}\text{Zn}_{0.025(1)}\text{Si}_4$ where the Zn content is at the level of an impurity. However, 0.12 at.% of Zn in the compound does appear as a significant value on the respective atomic site and qualitative EDX measurements confirmed the presence of Zn in the compound (see Figure S2, Supporting

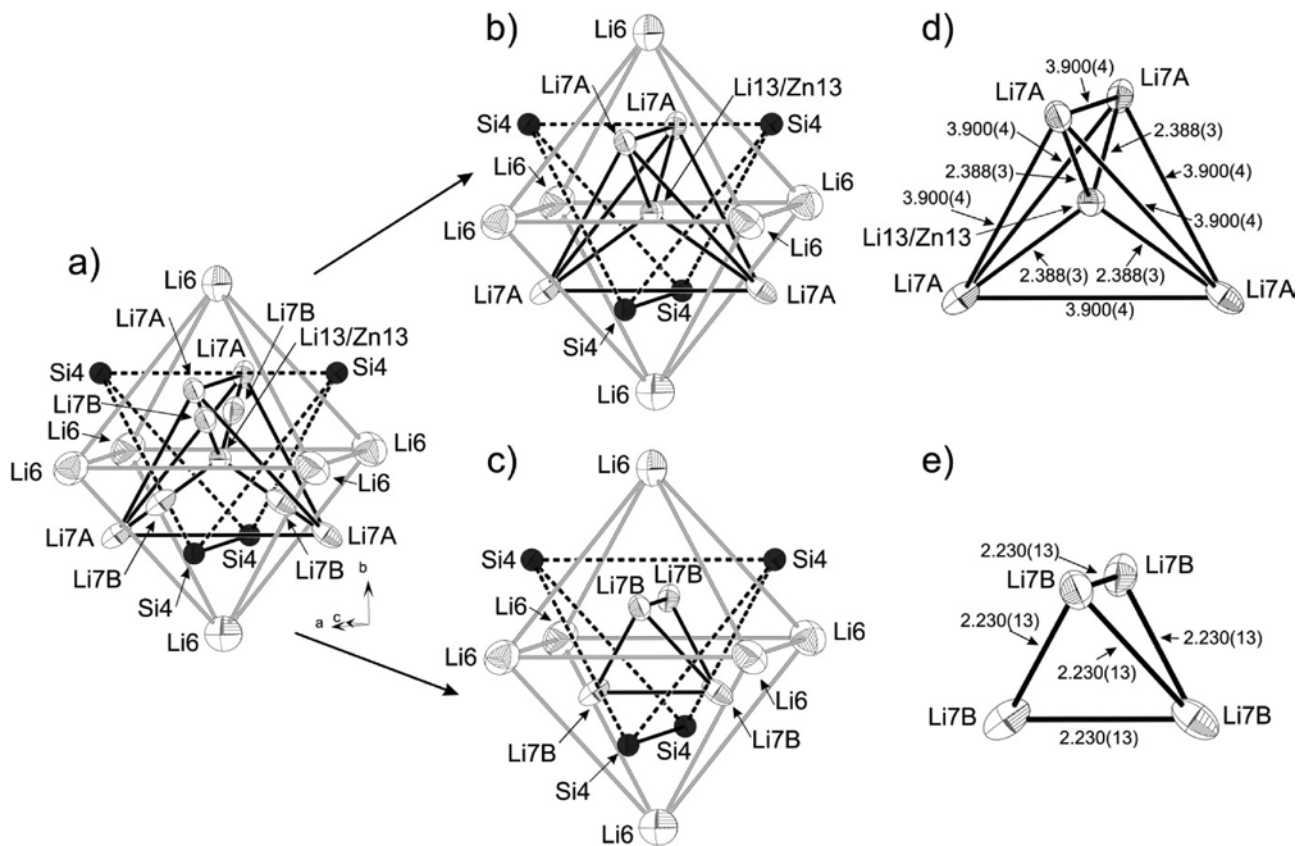


Fig. 1: Coordination of the atomic site $4a$ and split model for the atom $\text{Li}7$. (a) Coordination of the atomic site $4a$; (b) the situation with $\text{Li}7\text{A}$ atoms; (c) the situation with $\text{Li}7\text{B}$ atoms; (d)–(e) distances between the $4a$ site and the $\text{Li}7\text{A}$ or $\text{Li}7\text{B}$ atoms.

Information available online), but it was not possible to determine the Zn amount precisely by this method. The anisotropic displacement parameters for the $\text{Li}13/\text{Zn}13$ site are about 2–3 times smaller than for other Li sites (Table 3) which also supports the idea of the presence of the heavier Zn atom at this site. The results are in line with the observation that $\text{Li}_{17}\text{Ge}_4$ also incorporates Zn under the formation of $\text{Li}_{17-\varepsilon}\text{Zn}_\varepsilon\text{Ge}_4$ ($\varepsilon=0.0052(12)$) [15], with a statistical Li/Zn mixture at the $4a$ atomic site (around 2.6% of Zn comparing to 12.4% for $\text{Li}_{17-\varepsilon}\text{Zn}_\varepsilon\text{Si}_4$). However, this site was fully occupied in the Ge compound, and a splitting of the neighboring atoms around the $4a$ site has not been observed.

Currently $\text{Li}_{17}\text{Si}_4$ is the Li-richest phase in the binary Li-Si phase diagram, and it has been shown that its crystal structure is closely related to another Li-rich phase, $\text{Li}_{21}\text{Si}_5$ [5]. In both compounds there are four sites of higher symmetry $4a$ (0, 0, 0), $4b$ (1/2, 1/2, 1/2), $4c$ (1/4, 1/4, 1/4), and $4d$ (3/4, 3/4, 3/4), which are all unoccupied for $\text{Li}_{21}\text{Si}_5$, but in which exclusively $4a$ is occupied in the model for $\text{Li}_{17}\text{Si}_4$. These special sites have a characteristic surrounding of neighboring atoms (Fig. 2a–d). The first shell consists of 4 Li atoms which form a tetrahedron. The next shell

contains either 4 Si atoms or 4 Li atoms which in both cases form tetrahedra. These two tetrahedra interpenetrate each other to give a star, which is enclosed by an octahedron of either Li or Si atoms.

As mentioned above, the site $4a$ in $\text{Li}_{17-\varepsilon}\text{Zn}_\varepsilon\text{Si}_4$ is occupied by a statistical Li/Zn mixture, and the positions are not fully occupied. The first shell of Li atoms around $4a$ (Fig. 2) is presented by tetrahedra formed by $\text{Li}7\text{A}$ and $\text{Li}7\text{B}$ atoms. The split model and the under-occupancy of $4a$ lead to a rather straightforward model: when the $\text{Li}7\text{B}$ atom site is occupied, the central $4a$ site remains empty as in Nesper's model for $\text{Li}_{21}\text{Si}_5$. When the $\text{Li}7\text{A}$ atom site is occupied, the $4a$ site is statistically occupied by Li/Zn. This reflects the $\text{Li}_{17}\text{Si}_4$ model and is analogous to the situation in $\text{Li}_{17-\varepsilon}\text{Zn}_\varepsilon\text{Ge}_4$.

4 Conclusion

After the undisputable structure determination of $\text{Li}_{17}\text{Si}_4$ some years ago, the question arises whether the closely related $\text{Li}_{21}\text{Si}_5$ exists as well. The difference between the two structures originates from the occupation of the

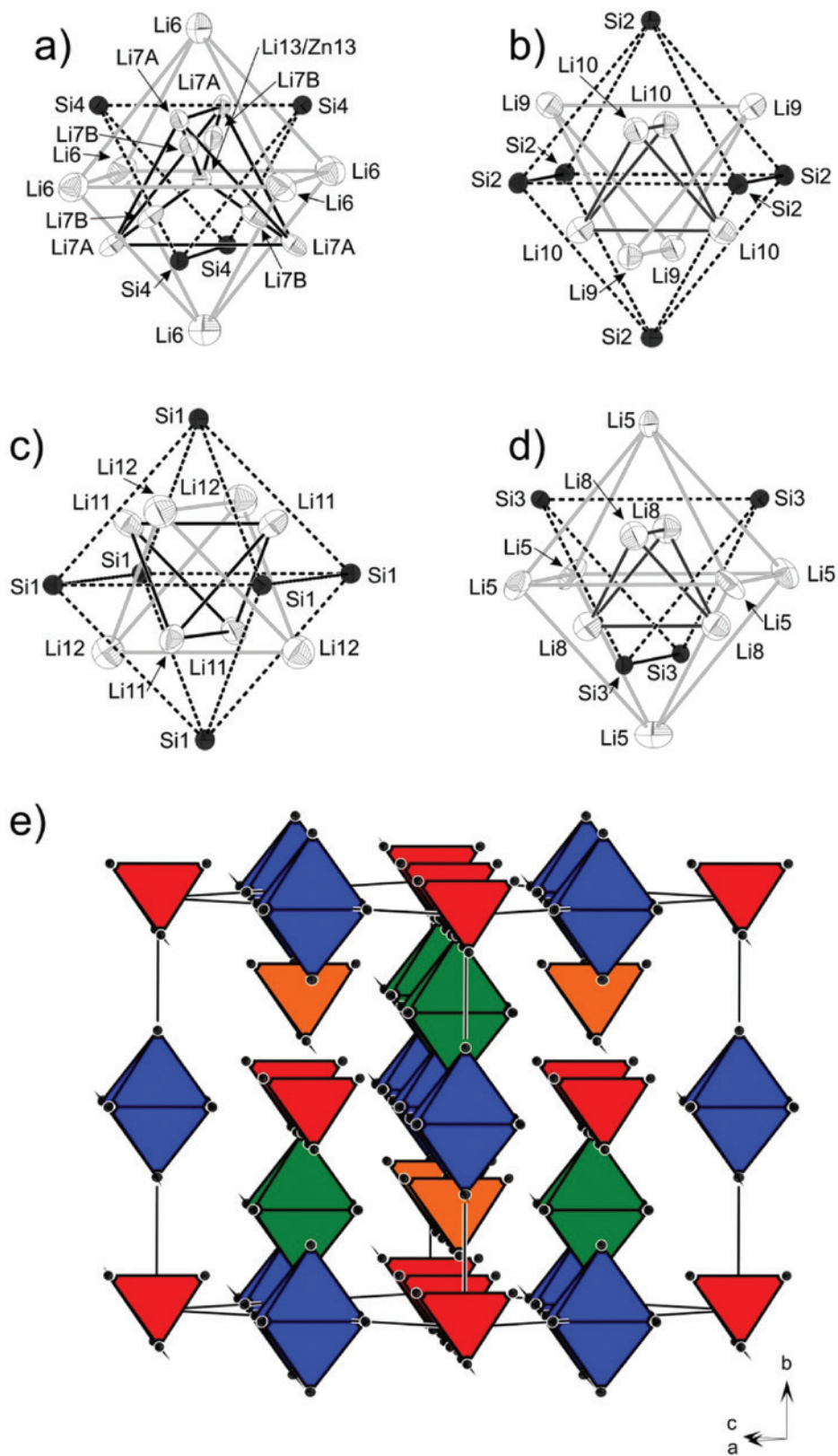


Fig. 2: Atomic shells with atom labels around the special positions in space group $\bar{F}43d$: (a) around the Li/Zn-filled site $4a$ (0, 0, 0); (b) around the unoccupied $4b$ site (1/2, 1/2, 1/2); (c) around the unoccupied site $4c$ (1/4, 1/4, 1/4); (d) around the unoccupied site $4d$ (3/4, 3/4, 3/4). (e) The NaTl-type arrangement of the Si polyhedra around the special positions $4a$, $4b$, $4c$, and $4d$ (marked in red, blue, green, and orange, respectively).

specific site 4a. Whereas $\text{Li}_{21}\text{Si}_5$, which an occupation of the 4a site with Li was not found in recent detailed investigations of the Li-rich side of the Li-Si phase diagram, we found now that in $\text{Li}_{17-\epsilon-\delta}\text{Zn}_\epsilon\text{Si}_4$ the site 4a is occupied by a mixture of Li and Zn and the occupation correlates with the occupation of neighboring atom sites. Thus the new ternary silicide $\text{Li}_{17-\epsilon-\delta}\text{Zn}_\epsilon\text{Si}_4$ shows the characteristics of $\text{Li}_{21}\text{Si}_5$ and can be considered as the missing link between the structures of $\text{Li}_{21}\text{Si}_5$ and $\text{Li}_{17}\text{Si}_4$.

5 Supporting information

Indexing of the X-ray powder pattern collected for $\text{Li}_{17-\epsilon-\delta}\text{Zn}_\epsilon\text{Si}_4$ and data of EDX measurements on single crystals of $\text{Li}_{17-\epsilon-\delta}\text{Zn}_\epsilon\text{Si}_4$ are given as supplementary material available online.

Acknowledgements: The authors thank Katia Rodewald for the EDX measurements of $\text{Li}_{17-\epsilon-\delta}\text{Zn}_\epsilon\text{Si}_4$.

References

- [1] A. Mukhopadhyay, B. W. Sheldon, *Prog. Mater Sci.* **2014**, *63*, 58–116.
- [2] C. Mao, M. Wood, L. David, S. J. An, Y. Sheng, Z. Du, H. M. Meyer, R. E. Ruther, D. L. Wood, *J. Electrochem. Soc.* **2018**, *165*, A1837–A1845.
- [3] M. Zeilinger, V. Baran, L. van Wüllen, U. Häussermann, T. F. Fässler, *Chem. Mater.* **2013**, *25*, 4113–4121.
- [4] V. Baran, L. van Wüllen, T. F. Fässler, *Chem. Eur. J.* **2016**, *22*, 6598–6609.
- [5] M. Zeilinger, D. Benson, U. Häussermann, T. F. Fässler, *Chem. Mater.* **2013**, *25*, 1960–1967.
- [6] R. Nesper, H. G. von Schnerring, *J. Solid State Chem.* **1987**, *70*, 48–57.
- [7] K. Puhakainen, M. Boström, T. L. Groy, U. Häussermann, *J. Solid State Chem.* **2010**, *183*, 2528–2533.
- [8] C. Lupu, J. G. Mao, J. W. Rabalais, A. M. Guloy, J. W. Richardson, *Inorg. Chem.* **2003**, *42*, 3765–3771.
- [9] APEX suite of crystallographic software, Bruker AXS Inc., Madison, WI (USA) **2008**.
- [10] SADABS, Bruker AXS Inc., Madison, WI (USA) **2008**.
- [11] SAINT, Bruker AXS Inc., Madison, WI (USA) **2008**.
- [12] G. M. Sheldrick, *SHELXS-97*, Program for the Solution of Crystal Structures, University of Göttingen, Göttingen (Germany) **1997**.
- [13] G. M. Sheldrick, *SHELXL-2014*, Program for Crystal Structure Refinement, University of Göttingen, Göttingen (Germany) **2014**.
- [14] A. F. Wells, *Structural Inorganic Chemistry*, Clarendon Press, Oxford, **1984**.
- [15] L. Lacroix-Orio, M. Tillard, C. Belin, *J. Alloys Compd.* **2008**, *465*, 47–50.

Supplementary Material: The online version of this article offers supplementary material (<https://doi.org/10.1515/znb-2019-0157>).